

Geophysical Research Letters

RESEARCH LETTER

10.1029/2018GL079094

Key Points:

- Mean-normalized wetland area and perimeter distributions are similar across the United States, despite hydroclimate and landscape differences
- Wetland areas and perimeters estimated from DEMs show good agreement with imagery-based data from the U.S. National Wetland Inventory
- Wetland shoreline fractal dimension estimated from perimeter/area ratios varies within the range [1, 1.5] but is clustered around 4/3 and reflects the typical landscape value

Supporting Information:

- Supporting Information S1

Correspondence to:

A. F. Aubeneau,
aubeneau@purdue.edu

Citation:

Bertassello, L. E., Rao, P. S. C., Jawitz, J. W., Botter, G., Le, P. V. V., Kumar, P., & Aubeneau, A. F. (2018). Wetlandscape fractal topography. *Geophysical Research Letters*, 45, 6983–6991. <https://doi.org/10.1029/2018GL079094>

Received 5 JUN 2018

Accepted 30 JUN 2018







Accepted article online 11 JUL 2018

Published online 24 JUL 2018

Corrected 30 AUG 2019

This article was corrected on 30 AUG 2019. See the end of the full text for details.

Wetlandscape Fractal Topography

Leonardo E. Bertassello¹ , P. Suresh C. Rao^{1,2}, James W. Jawitz³ , Gianluca Botter⁴ ,
Phong V. V. Le^{5,6} , Praveen Kumar⁵ , and Antoine F. Aubeneau¹ 

¹Lyles School of Civil Engineering, Purdue University, West Lafayette, IN, USA, ²Agronomy Department, Purdue University, West Lafayette, IN, USA, ³Soil and Water Sciences Department, University of Florida, Gainesville, FL, USA, ⁴Department of Civil, Architectural and Environmental Engineering, University of Padua, Padua, Italy, ⁵Department of Civil and Environmental Engineering, University of Illinois at Urbana-Champaign, Urbana, IL, USA, ⁶Faculty of Hydrology Meteorology and Oceanography, Vietnam National University, Hanoi, Vietnam

Abstract Natural wetlands are ecological, biogeochemical, and hydrological hot spots yet continue to disappear under human pressure. Their shapes and sizes control their hydroecological functions. We propose that elevation data can be used to delineate potential wetlands and that the (statistical) distributions of potential wetlands should be identical to the distributions of actual wetlands. We compare the shape and size distributions of wetlands reported in the National Wetland Inventory with those of potential wetlands identified using a topographic depression identification model. We estimated area and perimeter distributions as well as shoreline fractal dimension in six contrasting locations in the United States. Pareto distributions described the tails of these distributions, with similar slopes for both model and data. The shape of shorelines was also similar, and their fractal dimension clustered around $D = 4/3$, a pervasive value in nature. We also analyzed the entire wetland inventory data set for the conterminous United States (~20 million wetlands) for reference and found the statistics to be invariant across scales. Our results demonstrate that a simple topographic model can identify most reported wetlands as well as potential wetlands missing from the inventory. These findings could inform strategic surveys and the conservation of wetlandscapes.

Plain Language Summary Wetlands provide important hydrological and ecological services. Their diverse sizes and shapes control the amount of water they can hold and the species they can harbor. Because water accumulates at low elevation, we proposed that topography alone can reveal the location of wetlands. We also hypothesized that the (statistical) distribution of the (potential) wetlands identified from elevation data would be identical to the distribution of actual wetlands. We used a topographic depression identification model to delineate potential wetlands in six 10×10 km landscapes across the United States and compared the modeled wetlands to real wetlands cataloged in the National Wetland Inventory. The distribution of shapes and sizes were similar for both potential and real wetlands, indicating that topography data alone can be used to identify wetlands' properties. Widely available elevation data may thus be used to guide surveying and management when inventories are scarce. The scaling of area and perimeter distributions was similar across the six contrasting locations we analyzed and across scales (10×10 km, 30×30 km, and conterminous United States). The apparent universality of the observed scaling could help managers and stakeholders preserve the fundamental properties of wetlandscapes.

1. Introduction

Wetlands play an important role in watershed hydrology, affecting water storage, flow generation, ground-water dynamics, and evapotranspiration (Bullock & Acreman, 2003; Rains et al., 2016). Wetlands are also hot spots of nutrient retention and transformation, sediment storage, and biodiversity (Cheng & Basu, 2017; Cohen et al., 2016; Euliss et al., 2004; Reddy et al., 1999). The U.S. Clean Water Act defines wetlands as “areas that are inundated or saturated by surface or ground water at a frequency and duration sufficient to support [...] a prevalence of vegetation typically adapted for life in saturated soil conditions.” Delineation of wetlands is thus challenging because their boundaries are dynamic in both space and time (inundation, erosion, size of surrounding ecotone, etc.). Since the definition of wetlands requires inundation, we propose that topographic information alone is sufficient to identify potential wetlands.

Wetland ecohydrological functions are closely tied to their morphological characteristics (Biggs et al., 1994; Brooks & Hayashi, 2002; Cole & Brooks, 2000). The study of wetland shorelines is important from a

hydrological perspective because the exchange of surface water and groundwater occurs mostly along these edges and increases with the ratio of perimeter to area (Millar, 1971). The transitional habitats at the edges are also hot spots of diversity, and wetland morphological attributes thus prescribe ecological services. Moreover, wetlands embedded in the landscape serve as a mosaic of networked habitats. Maintaining the diverse sizes and shapes of wetlands could sustain habitat connectivity and biodiversity (Gibbs, 2000; Whigham, 1999), as well as hydrological and biogeochemical functions (Cohen et al., 2016; Rains et al., 2016). Restoration efforts could focus on conserving these distributions in landscapes to maximize benefits (Van Meter & Basu, 2015). We suggest that the statistical distributions of the sizes and shapes of actual wetlands can be obtained from those of potential wetlands.

Landscape features are fractal, and their (fractal) dimension encapsulates their (irregular) geometry (Mandelbrot, 1983; Sugihara & May, 1990; Turcotte, 1997). Fractal dimensions could thus describe the distinct patterns of isolated (Cohen et al., 2016) or networked (Larsen & Harvey, 2010) wetlands in wetlandscapes (landscapes characterized by an abundance of wetlands). Ensembles of natural objects are also often fractal, exhibiting scaling properties reflected in their statistical distributions. In this study, we use fractal analyses to compare wetlands from a model (topography depression identification (TDI) Le & Kumar, 2014) and a database (the U.S. National Wetland Inventory [NWI]). We estimated the fractal dimension (D) and probability distributions of area (A) and perimeter (P) of modeled and real wetlands. We chose six disparate wetlandscapes in the United States and compared the TDI model output with data provided by the NWI. We also include the analysis of the entire NWI database (excluding riverine and coastal wetlands because they track lines) by comparing local ($\sim 100 \text{ km}^2$) and continental scales (conterminous United States). Discrepancies between model estimates and data reveal the influence of other important factors not integrated in TDI. For example, the TDI model could identify depressions as potential wetlands in arid climates that cannot sustain hydrophytes. Conversely, potential wetlands may indicate actual wetlands not listed in the inventory, for example, wetlands that are too small to be identified or former wetlands drained after land use change. Nevertheless, the comparison between the TDI model and NWI data is important to assess whether widely available digital elevation models (DEMs) may be used to guide wetland surveys and management.

2. Methods

2.1. Geospatial Data and Six Case Study Wetlandscapes

We selected six $10 \times 10 \text{ km}$ landscapes in the conterminous United States (Figure 1) that have an abundance of wetlands to represent a wide range of environments with diverse wetland types, such as vernal pools (California and Maine), cypress domes (Florida), prairie potholes (North Dakota), basin wetlands (Minnesota), and playa lakes (Texas). The landscapes located in Florida, North Dakota, and Texas are mainly characterized by a flat topography and a larger presence of geographically isolated wetlands, while the landscapes located in California, Maine, and Minnesota exhibit a larger variation in the elevation profile, and some of the wetlands are affected by the presence of river networks. Hydroclimatic differences in these regions are described by the aridity index (AI; supporting information Table S2), defined as the ratio of the mean annual actual evapotranspiration (AET) to mean annual rainfall (P ; Sanford & Selnick, 2013). Texas and North Dakota represent the driest regions (high AI), while Maine and Minnesota are wet (low AI). Dominant land cover is also heterogeneous in the six regions: natural vegetation such as grassland, scrublands, and woodlands in California and Florida, croplands, forests, and woodlands in Maine and Minnesota, croplands in North Dakota, and croplands with patches of scrublands and grasslands in Texas (Homer et al., 2015).

The DEM data from the United States Geological Survey (USGS) National Map Viewer (<https://viewer.nationalmap.gov>) were used in our analysis. The DEM data are of $1/3$ arc-second resolution ($\sim 10 \times 10 \text{ m}$). Actual wetland data were obtained from the NWI (<https://www.fws.gov/wetlands/>) for the six landscapes, and we considered all wetlands larger than 100 m^2 for consistency with the DEM resolution. We also extended our analyses to $30 \times 30 \text{ km}$ grids to assess whether the results would change with scale (supporting information—Text S3). Finally, we examined the perimeter and area distributions, as well as shoreline fractal dimension of all wetlands (excluding riverine and estuarine) listed in the NWI database (~ 20 million) to compare with the six test areas.

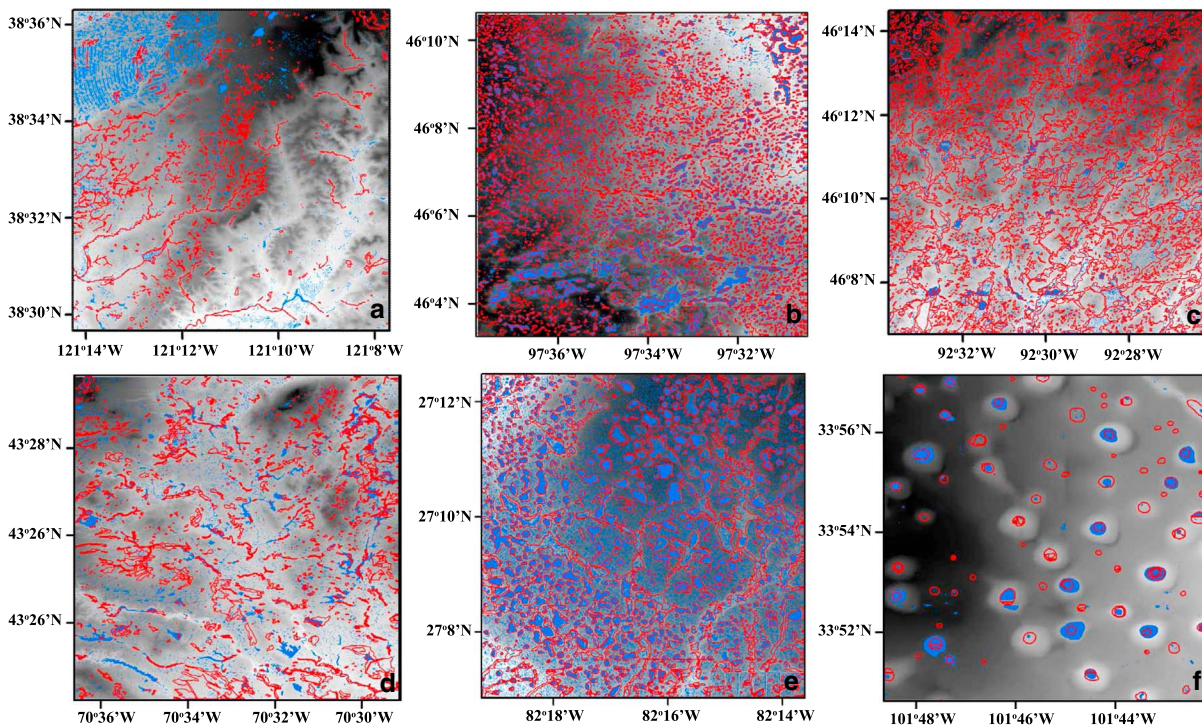


Figure 1. Representation of the digital elevation model (grayscale background) of six 10×10 km landscapes and actual wetlands (red lines) from the National Wetland Inventory database: California vernal pools (a), North Dakota prairie potholes (b), Minnesota basin wetlands (c), Maine vernal pools (d), Florida cypress domes (e), and Texas playa lakes (f). The blue polygons represent the potential wetlands identified by the topographic depression identification model.

2.2. Wetland Identification Using DEM

Wetland identification is challenging because their morphological properties (area and shape) change with flooding, vegetation, and soil conditions (Tiner, 2016). In our analysis, we applied a DEM-based approach to delineate potential wetlands as landscape units defined by elevation. To identify such wetlands, we followed the recent framework developed by Chu et al. (2010), Shaw et al. (2012), and Chu et al. (2013) and improved by Le and Kumar (2014). The TDI model considers the centers of potential wetlands as the local minima across the landscape determined by applying the D8 algorithm proposed by O'Callaghan and Mark (1984). Starting from these low elevations, a local-search algorithm identifies the neighboring cells pertaining to a depression (Chu et al., 2010) and ends once a threshold is identified. This threshold represents the highest elevation for water ponding, beyond which water spills. At the threshold level, a wetland reaches its maximum stage, area, and storage volume. The elevation of the wetland threshold (local maxima in the landscape) controls the shift from wetland-filling to wetland-spilling and/or merging (Chu et al., 2013).

The TDI model considers all depressions in which water can accumulate as wetlands and simulates the filling of the landscape with water. The DEM is edited by raising the depression cell to the threshold level (l). The algorithm is then implemented again to derive the maximum values for stage, surface area, perimeter, and storage volume of the wetlands for the next level of filling (l_{n+1}). Following Chu et al. (2010) and Le and Kumar (2014), geometric attributes of wetlands were estimated from the output of the TDI model. The surface area, $A_k^{(l)}$ [L^2], of the k th depression at level l is the sum of the areas of all individual cells within that depression, while the wetland perimeter is the sum of the distance between each adjoining pair of pixels around the border of the region. Therefore, when the threshold level, l , is low, the landscape is mainly composed of small and shallow wetlands, while for higher l , the degree of wetness of the landscape increases because wetlands are getting bigger and they can spill over large areas and merge (Supporting Information Text S1).

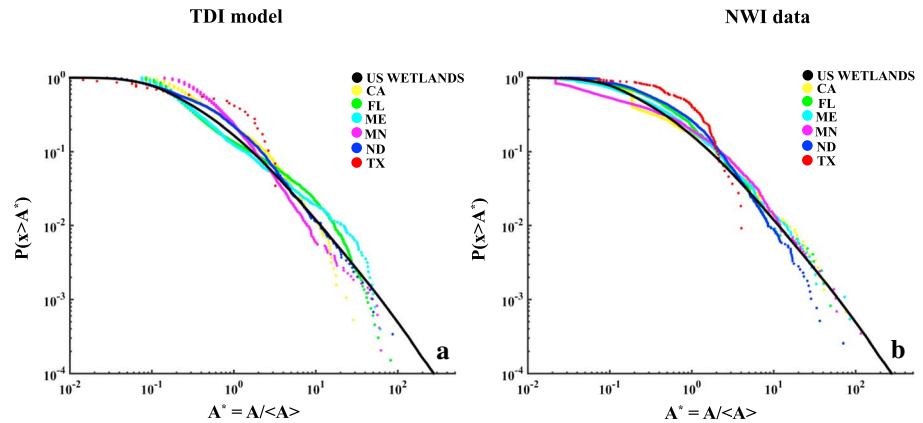


Figure 2. Comparison between the normalized wetland size distributions, A^* , obtained from the TDI model (a) and the NWI database (b) for the six wetlandscapes. A represents wetlands' area and $\langle A \rangle$ the mean wetland area in that landscape. In both plots we reported the wetland size distribution for all the U.S. wetlands (black solid line) obtained from the entire NWI database (except riverine and coastal). The tail of this distribution continues for four additional orders of magnitude of probability (supporting information—Text S4). The comparison between the output of the TDI model and the NWI data for the normalized perimeter is reported in Figure S17 in the supporting information. TDI = topographic depression identification; NWI = National Wetland Inventory.

2.3. Evaluation of Fractal Dimensions

The complexity in the geometry of wetland boundaries is evaluated using shoreline fractal dimension, D , determined based on the relationship between wetland perimeter, P , and area, A (Krummel et al., 1987; Mandelbrot, 1975; Sugihara & May, 1990):

$$P = kA^{\frac{D}{2}} \quad (1)$$

where k is a proportionality factor. For circles, $P \propto \sqrt{A}$ and $D = 1$. For more complex shapes, the perimeter becomes increasingly dissected (plane filling) or elongated (e.g., riverine wetlands), resulting in the limit in linear shapes where $P \sim A$ and $D = 2$. Natural wetlands span the spectrum of shapes between lines and circles.

The wetland shoreline fractal dimension was determined here from $D = 2r$, where r is the slope of the regression line of the log-transformed equation (1). We compared the results obtained from the regression between the $\log(P)$ and $\log(A)$ of the potential wetlands (TDI) and the NWI wetlands (supporting information—Text S2). For the TDI model, wetland shorelines are constrained by the elevation profile at the prescribed threshold level, l . For the NWI, wetland shorelines are determined by on-screen interpretation of digital imagery (Tiner, 2016). The procedures used to produce the NWI data also consider the presence of vegetation at the interface between wetland-upland area and soil moisture (Dahl, 1990).

3. Results

3.1. Wetland Area Distributions

We first compared the complementary cumulative distribution functions (ccdfs) of the TDI results and the NWI data. Plots of wetland area ccdfs, scaled by the mean area in each wetlandscapes, are shown in Figures 2a and 2b both for the TDI model and the NWI data. Because the abundance of small wetlands is uncertain (Lehner & Döll, 2004; Seekell & Pace, 2011), we fitted a Pareto distribution ($P(X > x) \propto x^{-\alpha}$) to the ccdf tails starting at a value x_{\min} representing the lower bound of the power law behavior (Clauset et al., 2009). Both α and x_{\min} were estimated via maximum likelihood. We also report the goodness of fit of the power law as a Kolmogorov-Smirnov statistic. The results (Tables 1 and S2) show that the estimates from both TDI model and NWI data are consistent. Indeed, the 95% confidence interval for the α scaling exponent overlap in each distribution. The p values reported in Table 1 refer to the probability that an artificial Pareto distribution is different from the observed sample data distribution. Larger p values thus suggest that the two distributions are not statistically different, or that the tails of the distributions are

Table 1
Estimation of the Exponent of the Power Law for the Wetland Size Distributions in the Six 10 × 10 km Wetlandscapes

Wetlandscape locations	TDI model			NWI data			AI
	α	x_{\min}	p value	α	x_{\min}	p value	
CA	1.69 ± 0.12	2.34	0.64	1.53 ± 0.02	2.89	0.48	0.5–0.59
FL	1.08 ± 0.11	0.67	0.41	1.38 ± 0.09	1.51	0.53	0.65–0.75
ME	1.21 ± 0.13	0.62	0.24	1.27 ± 0.03	1.86	0.25	0.4–0.49
MN	1.62 ± 0.03	2.49	0.84	1.71 ± 0.06	2.08	0.41	0.5–0.59
ND	1.57 ± 0.08	2.25	0.92	1.67 ± 0.12	2.44	0.69	0.8–0.89
TX ^a	3.11 ± 0.16	1.69	0.31	3.16 ± 0.12	1.59	0.91	0.95–1.05
COM	1.32 ± 0.03	1.78	0.58	1.36 ± 0.05	1.91	0.34	

Note. The scaling exponent, α , is estimated via the method of maximum likelihood. In addition, we perform a goodness-of-fit test of the power law based on the Kolmogorov-Smirnov statistic (Clauset et al., 2009), showing the 95% confidence interval for the scaling exponent. The p value is reported (high p value means that the observed distribution is not different from an artificial Pareto distribution with the same exponent). The x_{\min} value is the lower limit of the power law behavior. AI refers to the aridity index that characterizes the studied region (Sanford & Selnick, 2013). The acronym COM stands for the combined data set of the six case studies into a single distribution. A similar table for the scaling exponent of the wetland perimeter distribution, α , is reported as Table S2 (supporting information). TDI = topography depression identification; NWI = U.S. National Wetland Inventory; CA = California; FL = Florida; ME = Maine; MN = Minnesota; ND = North Dakota; TX = Texas.

^aTexas does not provide a robust estimate since it is composed of too few wetland data.

power law distributed. We also fitted the combined data set of the six case studies into a single distribution. The Pareto scaling exponents, α , for the TDI model ($\alpha = 1.32$, $x_{\min} = 1.78$) and NWI data ($\alpha = 1.36$, $x_{\min} = 1.91$) were not statistically different ($p > 0.05$), suggesting that the TDI model is an acceptable predictor of the larger wetland distribution. We also ran the TDI model and analyzed the NWI data on 30 km × 30 km grids encompassing our original wetlandscapes, showing that the results are independent of sample size (supporting information—Text S3). The scaling exponents of wetland areas are the same in these larger landscapes.

Figures 2a and 2b also show the area distribution for all the wetlands listed in the NWI for conterminous United States (black solid line), excluding the riverine and estuarine waterbodies. The normalized ccdf of the areas of all the wetlands in the NWI data set lines up with that of the 100-km² subsets we analyzed here. The Pareto tail ($\alpha = 1.42$, $x_{\min} = 2.05$) was truncated for legibility but continues for several more orders of magnitude to $A/\langle A \rangle \sim 10^4$ without obvious tempering before that point (Figures S11 and S12). The consistency between the TDI model and NWI area distributions determined from the 100-km² study sites and all the wetlands in the conterminous United States (excluding riverine and coastal) suggests that this scaling relation can be extended to larger wetlandscapes.

3.2. Wetlandscape Fractal Dimension

In the six wetlandscapes (Figures 3a and 3b) D values for all wetlands are distributed within the possible range [1, 2], from circle to lines. NWI data for the six wetlandscapes (Figure 3b) suggest several scaling regimes for D , bounded by circular shapes ($D = 1$) and riverine shapes (lines, $D = 2$), showing that not all riverine wetlands were censored during filtering. The shoreline fractal dimension is clustered around $D = 1.33$, which is the value corresponding to the unscreened perimeter of percolating clusters (Cael et al., 2015; Isichenko, 1992) as well as that of 2-D Brownian frontiers (Lawler et al., 2000; Mandelbrot, 1983). Larger water bodies appear constrained by a higher fractal dimension ($D = 1.5$), closer to that of the landscape itself (supporting information—Text S4).

Different wetland shapes are observed among and within wetlandscapes. For example, for wetlands in California, Maine, and Minnesota, we find $1 \leq D \leq 2$, while wetlands in Texas are mostly circular ($D \sim 1$). TDI estimates for the six wetlandscapes (Figure 3a) exhibit less variability in fractal dimension than the NWI data (Figure 3b). Riparian wetlands that are described by a large fractal dimension ($D \sim 2$) are not well identified by the TDI model because their shape tracks the rivers they flank and these wetlands are thus not delineated by elevation. The distributions of wetland shoreline fractal dimensions evaluated from the TDI and the NWI in the 100-km² test wetlandscapes are consistent with the shoreline fractal dimension evaluated for all the

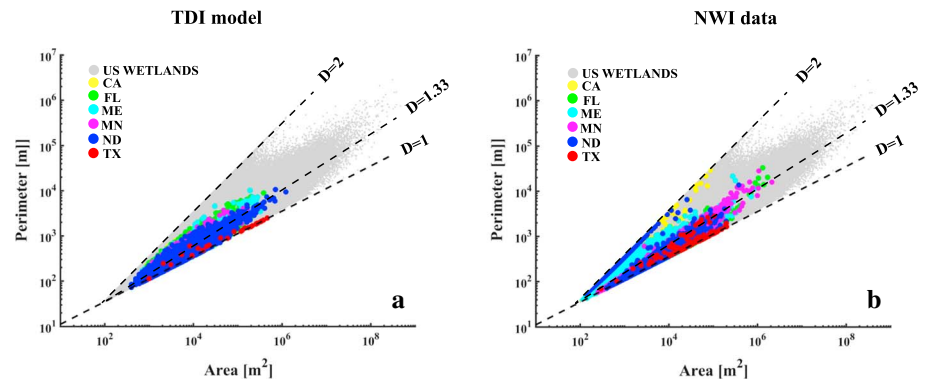


Figure 3. Shoreline fractal dimension D for the six wetlandscapes from the TDI model (a) and the NWI database (b). The black dashed lines represent scaling regimes for circular ($D = 1$) and linear ($D = 2$) wetlands. The $D = 1.33$ fractal dimension is evaluated from equation (1). The gray dots represent data from all the wetlands in the US (except riverine and coastal). TDI = topographic depression identification; NWI = National Wetland Inventory.

wetlands in the conterminous United States provided by the NWI database. This suggests that the 100-km² wetlandscapes are representative of the general patterns in the entire NWI database.

Fractal dimension links perimeter and area of a set of objects (equation (1)). Therefore, knowing the scaling exponent, α , of the wetland area distribution and the shoreline fractal dimension, D , we can predict the wetland perimeter Pareto scaling exponent $\beta = 2\alpha/D$ (Figures S17a and S17b in the supporting information), where $D = 1.33$. The estimated scaling exponents for the TDI ($\beta = 1.97$) and NWI data ($\beta = 2.02$) are consistent with the values obtained from maximum likelihood ($\beta = 1.95$, $x_{\min} = 2.98$ and $\beta = 1.98$, $x_{\min} = 2.09$, respectively). This procedure can also be extended to the entire NWI database (black lines in Figures S17a and S17b). In this case, $\beta = 1.89$ is the same as the estimates of the maximum likelihood method in the 10×10 -km wetlandscapes.

4. Discussion

We compared wetlands identified with a DEM-based approach (TDI) with actual wetlands from the NWI. High-resolution images and DEMs have long been used to extract geomorphic features from landscapes (Chu, 2017; Passalacqua et al., 2012; Wu & Lane, 2017). Our new method reproduced the sizes and shapes of actual wetlands, indicating that elevation models can be used to assess wetlands characteristics. The observed similarity between TDI model and data indicates that the morphological properties of wetlands are reflected in the elevation (DEM) data and identified by the TDI. Therefore, the abundance and possible locations of wetlands can be predicted in any other location on Earth where DEM data are available. The resolution of the DEM (10×10 m in our case) does not represent a limitation since it only affects the size of the smallest wetland that can be identified by the TDI method. Hence, even coarser DEMs may be suitable for this type of analysis. On the other hand, finer-resolution DEMs will improve the identification of smaller waterbodies as well as their contours.

The scaling of area and perimeter distributions was similar across the six contrasting locations we analyzed and across scales (10×10 km, 30×30 km, and conterminous United States). Apparent universality of the observed scaling could provide a useful tool to managers and stakeholders. By targeting the conservation of wetlands distributions, agencies could maintain or improve the connectivity of distributed aquatic habitats in the landscape and their associated ecological services. These metapopulation conservation techniques have been used for centuries in game management in Europe and revived in the past decades following seminal studies of island biogeography and metapopulations (Levins, 1969; MacArthur & Wilson, 1967). Our analysis provides new evidence of their suitability for wetland conservation.

The TDI algorithm identifies small depressions (supporting information—Text S5) that are not included in the NWI data set. The NWI has well-documented limitations (Tiner, 1997), with omission errors underrepresenting small wetlands. Some of the wetlands may be completely dry or flooded depending on when the survey was made, since the hydrologic regime of smaller wetlands is driven by the stochastic hydroclimatic forcing

(Aquino et al., 2017; Shook et al., 2013; Zhang et al., 2009). In addition, the NWI could merge some of the small wetlands into larger complexes, since soil saturation and vegetation are criteria omitted in the TDI. We suggest that the TDI model can be used to identify small wetlands that are missing from inventories. We note however that not all the potential wetlands identified by the TDI model are necessarily actual wetlands in the landscape. For example, the TDI could identify depressions as potential wetlands even in arid climates that cannot support hydrophytes. In addition, closed depressions and flat areas on digital models of the land surface are sometimes artifacts (Martz & Garbrecht, 1992; Tribe, 1992). These features could be identified as potential wetlands by the TDI and increase the number of false positive (number of potential wetlands identified by the TDI model but not listed in the NWI database, Table S1). As such, for flat landscapes, the TDI is useful as a basis to inform wetland surveying but not as a definitive identification tool.

The shoreline fractal dimension of the actual wetlands, and those identified by the TDI model, are clustered around $D \sim 1.33$. This is similar to the classic $4/3$ scaling Mandelbrot conjectured for the frontiers of Brownian islands (Mandelbrot, 1983) and since proven by Lawler et al. (2000). This same value is also found from the perimeter-area relationship for lakes on Earth (Cael & Seekell, 2016) and Titan (Sharma & Byrne, 2010) and also is the average value for coastlines around the world (Mandelbrot, 1975). The NWI wetlands also show a small second peak around $D = 1.5$ not captured by the TDI (Figure S5). These more dissected contours may be missing from the TDI model because of limited DEM resolution. Pixelation becomes important when the object size is near the pixel size (Batista-Tomás et al., 2016), and thus the contour of small wetlands appears smoother (lower D) in the TDI output. However, the deviation from the $4/3$ dimension is more evident for larger wetlands (Figures 3a and 3b), which have more convoluted boundaries with fractal dimension closer to $D = 1.5$. This could be related to the dimension of the surface intersected. Our analysis of the 3-D landscape dimension shows typical values near 2.5 (supporting information—Text S4). An isoset (or zero set) intersecting the surface would thus have a dimension near 1.5 (Russ, 1994). We speculate that the consistently lower values observed in the shoreline fractal dimension for our six 100-km² test landscapes translate the local erosion at the wetland boundary with the diffusive, mass-wasting erosive processes leading to smoother than expected contours. For the larger wetlands, however, the actual topography of the terrain may constrain the shoreline, as reflected in their (higher) dimension.

Fractal dimension is useful to evaluate and interrogate the spatial heterogeneity associated with the genetic processes that shaped the wetlandscapes. Wetlands formed by similar processes should have similar shapes and thus the same fractal dimension. For example, wind carved the Texas playa, hollowing out depressions in dry, noncohesive soils down to the local water table (Tiner, 2016), resulting in the typical rounded shapes we observed. The postglaciation receding ice sheets shaped the glaciolacustrine plains of North Dakota (Figure 1b) or Minnesota (Figure 1c; Kantrud et al., 1989). Limestone dissolution strongly affected the formation of the Florida cypress domes (Figure 1e). Still in Florida, the Everglades exhibit these peculiar parallel ridge and slough patterns (Larsen & Harvey, 2010). Each particular process results in a particular shape associated with a particular fractal dimension. We suggest that our results could support further analysis and classification. For example, the size beyond which circular shapes do not exist and the scaling regime appears to shift could reveal the local interaction of land and climate.

5. Conclusions

We presented a DEM-based approach for the identification of potential wetlands. The distributions of sizes and shapes obtained from the model were similar to those observed in nature. The TDI model identified small wetlands not inventoried and could be used to inform wetland surveying. This approach is geographically transferable and may be especially valuable in areas where synoptic data are sparse or not available. We also showed that properties scale from small regions to the continent, and therefore our analysis could be performed efficiently for diverse locations. Complex interactions of land and climate that prescribe wetlands are embedded in their scaling properties, which in turn control their ecohydrological functions. Our results could thus inform efforts to preserve or restore the fundamental properties of wetlandscapes.

References

- Aquino, T., Aubeneau, A., McGrath, G., Bolster, D., & Rao, P. S. C. (2017). Noise-driven return statistics: Scaling and truncation in stochastic storage processes. *Scientific Reports*, 7(1), 302. <https://doi.org/10.1038/s41598-017-00451-x>

Acknowledgments

We thank M. B. Cardenas, V. Ivanov, B. B. Cael, and an anonymous reviewer for their comments on earlier versions of the manuscript. Lee A. Rieth Endowment in the Lyles School of Civil Engineering at Purdue University provided partial financial support for this research. The DEM data used in this analysis were obtained from the United States Geological Survey (USGS) National Map Viewer (<https://viewer.nationalmap.gov>), while actual wetland data were obtained from the NWI (<https://www.fws.gov/wetlands/>).

- Batista-Tomás, A. R., Díaz, O., Batista-Leyva, A. J., & Altshuler, E. (2016). Classification and dynamics of tropical clouds by their fractal dimension. *Quarterly Journal of the Royal Meteorological Society*, 142(695), 983–988. <https://doi.org/10.1002/qj.2699>
- Biggs, J., Corfield, A., Walker, D., Whitfield, M., & Williams, P. (1994). New approaches to the management of ponds. *British Wildlife*, 5, 273–287.
- Brooks, R. T., & Hayashi, M. (2002). Depth-area-volume and hydroperiod relationships of ephemeral (vernal) forest pools in southern New England. *Wetlands*, 22, 247. [https://doi.org/10.1672/0277-5212\(2002\)022](https://doi.org/10.1672/0277-5212(2002)022)
- Bullock, A., & Acreman, M. (2003). The role of wetlands in the hydrological cycle. *Hydrology and Earth System Sciences*, 7(3), 358–389. <https://doi.org/10.5194/hess-7-358-2003>
- Cael, B. B., Lambert, B., & Bisson, K. (2015). Pond fractals in a tidal flat. *Physical Review E*, 92(5), 052128. <https://doi.org/10.1103/PhysRevE.92.052128>
- Cael, B. B., & Seekell, D. A. (2016). The size-distribution of Earth's lakes. *Scientific Reports*, 6(1), 29633. <https://doi.org/10.1038/srep29633>
- Cheng, F. Y., & Basu, N. B. (2017). Biogeochemical hotspots: Role of small water bodies in landscape nutrient processing. *Water Resources Research*, 53, 5038–5056. <https://doi.org/10.1002/2016WR020102>
- Chu, X. (2017). Delineation of pothole-dominated wetlands and modeling of their threshold behaviors. *Journal of Hydrologic Engineering*, 22(1), D5015003–D5015011. [https://doi.org/10.1061/\(ASCE\)HE.1943-5584.0001224](https://doi.org/10.1061/(ASCE)HE.1943-5584.0001224)
- Chu, X., Yang, J., Chi, Y., & Zhang, J. (2013). Dynamic puddle delineation and modeling of puddle-to-puddle filling-spilling-merging-splitting overland flow processes. *Water Resources Research*, 49, 3825–3829. <https://doi.org/10.1002/wrcr.20286>
- Chu, X., Zhang, J., Chi, Y., & Yang, J. (2010). In K. W. Potter, & D. K. Frevert (Eds.), *An improved method for watershed delineation and computation of surface depression storage, in Watershed Management 2010: Innovations in watershed management under land use and climate change, chap. 99* (pp. 1113–1122). Reston, VA: American Society of Civil Engineers. [https://doi.org/10.1061/41143\(394\)100](https://doi.org/10.1061/41143(394)100)
- Clauset, A., Shalizi, C., & Newman, M. (2009). Power-law distributions in empirical data. *SIAM Review*, 51(4), 661–703. <https://doi.org/10.1137/070710111>
- Cohen, M. J., Creed, I. F., Alexander, L., Basu, N. B., Calhoun, A. J., Craft, C., et al. (2016). Do geographically isolated wetlands influence landscape functions? *Proceedings of the National Academy of Sciences of the United States of America*, 113(8), 1978–1986. <https://doi.org/10.1073/pnas.1512650113>
- Cole, C. A., & Brooks, R. P. W. (2000). Patterns of wetland hydrology in the Ridge and Valley Province. *Pennsylvania, USA*, 20, 438. [https://doi.org/10.1672/0277-5212\(2000\)020](https://doi.org/10.1672/0277-5212(2000)020)
- Dahl, T. E. (1990). *Wetlands losses in the United States, 1780's to 1980's. Report to the Congress* (p. 13). Washington, DC: U.S. Department of the Interior; Fish and Wildlife Service.
- Euliss, N. H., LaBaugh, J. M., Fredrickson, L. H., Mushet, D. M., Laubhan, M. K., Swanson, G. A., et al. (2004). The wetland continuum: A conceptual framework for interpreting biological studies. *Wetlands*, 24(2), 448–458. [https://doi.org/10.1672/0277-5212\(2004\)024](https://doi.org/10.1672/0277-5212(2004)024)
- Gibbs, J. P. (2000). Wetland loss and biodiversity conservation. *Conservation Biology*, 14(1), 314–317. <https://doi.org/10.1046/j.1523-1739>
- Homer, C. G., Dewitz, J. A., Yang, L., Jin, S., Danielson, P., Xian, G., et al. (2015). Completion of the 2011 National Land Cover Database for the conterminous United States—Representing a decade of land cover change information. *Photogrammetric Engineering and Remote Sensing*, 81(5), 345–354.
- Isichenko, M. B. (1992). Percolation, statistical topography, and transport in random media. *Reviews of Modern Physics*, 64(4), 961–1043. <https://doi.org/10.1103/RevModPhys.64.961>
- Kantrud, H. A., Krapu, G. L., & Swanson, G. A. (1989). *Prairie basin wetlands of the Dakotas: A community profile, Biological Report 85(7.28)*, (). Washington, DC: U.S. Fish and Wildlife Service.
- Krummel, J., Gardner, R., Sugihara, G., O'Neill, R., & Coleman, P. (1987). Landscape patterns in a disturbed environment. *Oikos*, 48(3), 321–324. <https://doi.org/10.2307/3565520>
- Larsen, L., & Harvey, J. (2010). How vegetation and sediment transport feedbacks drive landscape change in the Everglades and wetlands worldwide. *The American Naturalist*, 176(3), E66–E79. <https://doi.org/10.1086/655215>
- Lawler, G. F., Schramm, O., & Werner, W. (2000). The dimension of the planar Brownian frontier is 4/3. arXiv: math/0010165.
- Le, P. V. V., & Kumar, P. (2014). Power law scaling of topographic depressions and their hydrologic connectivity. *Geophysical Research Letters*, 41, 1553–1559. <https://doi.org/10.1002/2013GL059114>
- Lehner, B., & Döll, P. (2004). Development and validation of a global database of lakes, reservoirs and wetlands. *Journal of Hydrology*, 296, 1–22. <https://doi.org/10.1016/j.jhydrol.2004.03.028>
- Levins, R. (1969). Some demographic and genetic consequences of environmental heterogeneity for biological control. *Bulletin of the Entomological Society of America*, 15(3), 237–240. <https://doi.org/10.1093/besa/15.3.237>
- MacArthur, R. H., & Wilson, E. O. (1967). *The theory of island biogeography*. Princeton, NJ: Princeton University Press.
- Mandelbrot, B. B. (1975). Stochastic models for the Earth's relief, the shape and the fractal dimension of coastlines, and the number-area rule for islands. *Proceedings of the National Academy of Sciences of the United States of America*, 72(10), 3825–3828. <https://doi.org/10.1073/pnas.72.10.3825>
- Mandelbrot, B. B. (1983). *The fractal geometry of nature*. New York: Freeman.
- Martz, L. W., & Garbrecht, J. (1992). Numerical definition of drainage network and subcatchment areas from digital elevation models. *Computational Geosciences*, 18(6), 747–761. [https://doi.org/10.1016/0098-3004\(92\)90007-E](https://doi.org/10.1016/0098-3004(92)90007-E)
- Millar, J. B. (1971). Shoreline-area ratio as a factor in rate of water loss from small sloughs. *Journal of Hydrology*, 14(3-4), 259–284. [https://doi.org/10.1016/0022-1694\(71\)90038-2](https://doi.org/10.1016/0022-1694(71)90038-2)
- O'Callaghan, J. F., & Mark, D. M. (1984). The extraction of drainage networks from digital elevation data. *Computer Vision Graphics Image Processing*, 28(3), 323–344. [https://doi.org/10.1016/S0734-189X\(84\)80011-0](https://doi.org/10.1016/S0734-189X(84)80011-0)
- Passalacqua, P., Belmont, P., & Fofoula-Georgiou, E. (2012). Automatic geomorphic feature extraction from lidar in flat and engineered landscapes. *Water Resources Research*, 48, W03528. <https://doi.org/10.1029/2011WR010958>
- Rains, M. C., Leibowitz, S. G., Cohen, M. J., Creed, I. F., Golden, H. E., Jawitz, J. W., et al. (2016). Geographically isolated wetlands are part of the hydrological landscape. *Hydrological Processes*, 30(1), 153–160. <https://doi.org/10.1002/hyp.10610>
- Reddy, K. R., Kadle, R. H., Flaig, E., & Gale, P. M. (1999). Phosphorus retention in streams and wetlands: A review. *Critical Reviews in Environmental Science and Technology*, 29(1), 83–146. <https://doi.org/10.1080/10643389991259182>
- Russ, J. C. (1994). *Fractal surfaces*. New York: Plenum.
- Sanford, W. E., & Selnick, D. L. (2013). Estimation of evapotranspiration across the conterminous United States using a regression with climate and land-cover data. *JAWRA Journal of the American Water Resources Association*, 49(1), 217–230. <https://doi.org/10.1111/jawr.12010>
- Seekell, D. A., & Pace, M. L. (2011). Does the Pareto distribution adequately describe the size-distribution of lakes? *Limnology and Oceanography*, 56(1), 350–356. <https://doi.org/10.4319/lo.2011.56.1.0350>

- Sharma, P., & Byrne, S. (2010). Constraints on Titan's topography through fractal analysis of shorelines. *Icarus*, *209*(2), 723–737. <https://doi.org/10.1016/j.icarus.2010.04.023>
- Shaw, D. A., Pietroniro, A., & Martz, L. (2012). Topographic analysis for the prairie pothole region of western Canada. *Hydrological Processes*, *27*, 3105–3114. <https://doi.org/10.1002/hyp.9409>
- Shook, K., Pomeroy, J. W., Spence, C., & Boychuk, L. (2013). Storage dynamics simulations in prairie wetland hydrology models: Evaluation and parameterization. *Hydrological Processes*, *27*(13), 1875–1889. <https://doi.org/10.1002/hyp.9867>
- Sugihara, G., & May, R. M. (1990). Applications of fractals in ecology. *Trends in Ecology & Evolution*, *5*(3), 79–86. [https://doi.org/10.1016/0169-5347\(90\)90235-6](https://doi.org/10.1016/0169-5347(90)90235-6)
- Tiner, R. W. (1997). NWI maps: What they tell us. *National Wetlands Newsletter*, *19*(2), 7–12.
- Tiner, R. W. (2016). *Wetland indicators: A guide to wetland formation, identification, delineation, classification, and mapping* (2nd ed.). Boca Raton, FL: CRC Press. ISBN 9781439853702
- Tribe, A. (1992). Automated recognition of valley lines and drainage networks from grid digital elevation models: A review and a new method. *Journal of Hydrology*, *139*(1–4), 263–293. [https://doi.org/10.1016/0022-1694\(92\)90206-B](https://doi.org/10.1016/0022-1694(92)90206-B)
- Turcotte, D. L. (1997). *Fractal and chaos in geology and geophysics*. Cambridge, UK: Cambridge University Press.
- Van Meter, K. J., & Basu, N. B. (2015). Signatures of human impact: Size distributions and spatial organization of wetlands in the prairie pothole landscape. *Ecological Applications*, *25*(2), 451–465. <https://doi.org/10.1890/14-0662.1>
- Whigham, D. (1999). Ecological issues related to wetland preservation, restoration, creation and assessment. *Science of the Total Environment*, *240*(1–3), 31–40. [https://doi.org/10.1016/S0048-9697\(99\)00321-6](https://doi.org/10.1016/S0048-9697(99)00321-6)
- Wu, Q., & Lane, C. R. (2017). Delineating wetland catchments and modeling hydrologic connectivity using lidar data and aerial imagery. *Hydrology and Earth System Sciences*, *21*(7), 3579–3595. <https://doi.org/10.5194/hess-21-3579-2017>
- Zhang, B., Schwartz, F. W., & Liu, G. (2009). Systematics in the size structure of prairie pothole lakes through drought and deluge. *Water Resources Research*, *45*, W04421. <https://doi.org/10.1029/2008WR006878>

Erratum

In the originally published version of this article, there was an error in the acknowledgments. This error has since been corrected, and the present version may be considered the authoritative version of record.